Arrays and Cascades of Fluorescent Liquid−Liquid Waveguides: Broadband Light Sources for Spectroscopy in Microchannels

Brian T. Mayers,[†] Dmitri V. Vezenov,[†] Valentine I. Vullev, and George M. Whitesides*

Department of Chemistry and Chemical Biology, Harvard University, 12 Oxford St., Cambridge, Massachusetts 02138

This paper describes the fabrication and operation of fluidic broadband light sources for use "on-chip" in integrated microanalytical systems. These light sources consist of liquid-core, liquid-cladding (L^2) microchannel waveguides with liquid cores containing fluorescent dyes, excited by incident light from an external halogen bulb. Simultaneous use of multiple fluorophores in a common solution, in a single L^2 light source, is not possible, because energy transfer from fluorophores emitting at shorter wavelength to fluorophores emitting at longer wavelength is essentially complete. Two approaches circumvent this problem of energy transfer; both use spatial separation of the fluorophores in different streams. The first setup uses a cascade (series) of single-core, single-dye light sources of increasing absorption energy to generate a combined broadband output. The second approach uses a parallel array of single-core, single-dye light sources. The spectral content of the light output for both cascade and array light sources can be controlled through choice of flow rates and dyes. Output intensity from these light sources is comparable to standard fiber-optic spectrophotometer light sources. The paper also discusses the efficiency of energy transfer between parallel liquid cores as a function of the fluid medium (index of refraction, path length, and rate of flow).

This paper describes a microfluidic, broadband light source that can, in principle, cover the entire spectrum required for spectroscopic applications in microanalysis. We explicitly address issues of energy transfer in solutions containing multiple fluorophores with overlapping absorption−emission bands.

Optical detection and spectroscopic analysis are important in most micrototal analysis systems (*μ*TAS).[1] The most commonly used methods for delivery of light to microchannels rely on the coupling of *external* sources of light to microfluidic devices (typically using optical fibers). This approach comes at the cost of aligning the fiber with the microfluidic system being examined, the need for multiple sources of light (in the case of cw lasers), and the limitations on design imposed by restrictions on the size and positions of the microchannels. We have recently described an integrated microfluidic fluorescent light source that circum-

vents many of these deficiencies by introducing a fluorescent dye into the liquid core of a liquid core/liquid cladding (L^2) waveguide:[2] the fluorescence emitted by the dye is guided within the core of the waveguide and propagated along the waveguide to the point of use.

Fluids have been used to transmit light in liquid-core/solid-cladding waveguides,[3−10] and liquid-core waveguides are commonly used to increase the optical path length of chip-based spectrophotometers.[11,12] Some optical characteristics of solid-core/liquid-cladding waveguides can be controlled in a dynamic fashion.[13−16] We have recently demonstrated full dynamic control of both the core and the cladding in fluid waveguides formed entirely by liquids flowing in the laminar regime in microfluidic devices (L^2 waveguides).[17] We chose to use L^2 waveguides for our fluorescent light sources for several reasons: (i) L^2 waveguides allow direct, dynamic control of optical and physical properties of both core and cladding; (ii) L^2 waveguides allow direct control over the sizes and geometries of the cores and claddings by manipulation of flow rate; (iii) L^2 waveguides fabricated in elastomers are inexpensive, amenable to rapid prototyping,[18−20]

(2) Vezenov, D. V.; Mayers, B. T.; Wolfe, D. B.; Whitesides, G. M. *Appl. Phys. Lett.,* in press.
(3) Schueller, O. J. A.; Zhao, X.-M.; Whitesides, G. M.; Smith, S. P.; Prentiss, M. *Adv. Mater.* **1999**, *11*, 37−41.
(4) Manor, R.; Datta, A.; Ahmad, I.; Holtz, M.; Gangopadhyay, S.; Dallas, T. *IEEE Sens. J.* **2003**, *3*, 687−692.
(5) Datta, A.; Eom, I.-Y.; Dhar, A.; Kuban, P.; Manor, R.; Ahmad, I.; Gangopadhyay, S.; Dallas, T.; Holtz, M.; Temkin, H.; Dasgupta, P. K. *IEEE Sens. J.* **2003**, *3*, 788−795.
(6) Dress, P.; Franke, H. *Appl. Phys. B* **1996**, *B63*, 12−19.
(7) Dijkstra, R. J.; Slooten, C. J.; Stortelder, A.; Buijs, J. B.; Ariese, F.; Brinkman, U. A. T.; Gooijer, C. *J. Chromatogr., A* **2001**, *918*, 25−36.
(8) Hanning, A.; Westberg, J.; Roeraade, J. *Electrophoresis* **2000**, *21*, 3290−3304.
(9) Wang, S.-L.; Huang, X.-J.; Fang, Z.-L.; Dasgupta, P. K. *Anal. Chem.* **2001**, *73*, 4545−4549.
(10) Liu, Z.; Pawliszyn, J. *Anal. Chem.* **2003**, *75*, 4887−4894.
(11) Dress, P.; Franke, H. *Rev. Sci. Instrum.* **1997**, *68*, 2167−2171.
(12) Olivares, J. A.; Stark, P. C.; Jackson, P. *Anal. Chem.* **2002**, *74*, 2008−2013.
(13) Domachuk, P.; Nguyen, H. C.; Eggleton, B. J.; Straub, M.; Gu, M. *Appl. Phys. Lett.* **2004**, *84*, 1838−1840.
(14) Mach, P.; Dolinski, M.; Baldwin, K. W.; Rogers, J. A.; Kerbage, C.; Windeler, R. S.; Eggleton, B. J. *Appl. Phys. Lett.* **2002**, *80*, 4294−4296.
(15) Kerbage, C.; Eggleton, B. J. *Appl. Phys. Lett.* **2003**, *82*, 1338−1340.
(16) Cattaneo, F.; Mach, P.; Hsieh, J.; Krupenkin, T.; Yang, S.; Rogers, J. A. *Mater. Res. Soc. Symp. Proc.* **2003**, *741*, 9−13.
(17) Wolfe, D. B.; Conroy, R. S.; Garstecki, P.; Mayers, B. T.; Fischbach, M. A.; Paul, K. E.; Prentiss, M.; Whitesides, G. M. *Proc. Natl. Acad. Sci. U.S.A.* **2004**, *101*, 12434−12438.
(18) Xia, Y.; Whitesides, G. M. *Annu. Rev. Mater. Sci.* **1998**, *28*, 153−184.
(19) McDonald, J. C.; Whitesides, G. M. *Acc. Chem. Res.* **2002**, *35*, 491−499.

* Corresponding author. E-mail: gwhitesides@gmwgroup.harvard.edu.
† These authors contributed equally to this work.

(1) Verpoorte, E. *Lab Chip* **2003**, *3*, 42N−52N.
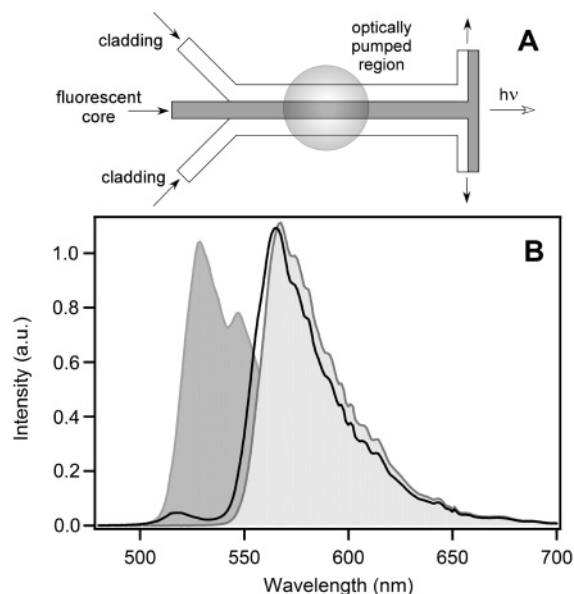
Figure 1. (A) Top-view scheme for the L^2 fluorescent light source, consisting of microfluidic channels in PDMS (n_D = 1.41). The dimensions of the central channel were 125 μm × 500 μm × 20 mm (h × w × l). The length of the waveguiding region was 2 cm. The optical pumping region was 4 mm in diameter. (B) The spectral output of a single-core L^2 fluorescent light source for three different dye solutions. Dark gray area, 1 mM fluorescein in EG (n_D = 1.431) in the core. Light gray area, 1 mM rhodamine 6G in EG in the core. Solid line, 0.5 mM of both fluorescein and rhodamine 6G in EG in the core. In each case, water (n_D = 1.331) was used as a cladding.

and compatible with microanalytical systems; (iv) L^2 waveguides are ideal for fluorescent light sources, because fluorescent dyes can continuously flow through the waveguide, thus limiting the effects of bleaching.

Spectroscopy often requires a greater range of wavelengths than can be produced by a single fluorescent organic dye (which usually has a bandwidth of emission on the order of 50 nm).[21] In principle, simultaneous emission from several organic dyes with adjacent emission bands could cover an arbitrary range of wavelengths in the UV, visible, and near-IR spectrum. Energy transfer from a dye emitting at short wavelength to one emitting at long wavelength (due both to absorption−reemission and to resonance energy transfer)[22] limits the usefulness of multiple fluorescent dyes in a common solution (Figure 1). To resolve the problem of quenching through energy transfer, the dyes must be separated either (i) in energy or (ii) in space. The first approach requires the use of fluorophores with no overlap between emission and adsorption of the different dyes. The second method avoids absorption of emitted fluorescence by collecting the emission of each dye in spatially distinct, nonoverlapping regions. We believed that the second approach−spatial separation of emitting waveguides−is the more practical of the two, because it does not require exotic fluorophores[23] or high-energy (UV) pump sources for microfluidic applications. We take advantage of the laminar

flow regime in microfluidic systems[24] and demonstrate that arrays and cascades of L^2 waveguides are a natural choice for spatial confinement of individual fluorescent light sources; these sources can then be combined, serially or in parallel, for broadband output.

MATERIALS AND METHODS

Microchannels. Photoresist-on-Si masters of the microchannels were prepared in a clean room with photolithography (Micro-Chem, SU-8 100) using transparency masks (CAD/Art Services, Inc., Poway, CA). Microchannels were fabricated with poly-(dimethylsiloxane) (PDMS) using standard polymer replica molding procedures[18,19] and sealed against flat pieces of PDMS after plasma oxidation. The height of all of the channels used in these experiments was ∼130 μm. The height was the minimum required to allow insertion of a 105-μm core/125-μm-diameter multimode optical fiber (step-index, numerical aperture 0.22) to couple the waveguide output to a spectrometer. For spectroscopic measurements, L^2 devices were prepared with an open-ended, 150-μm microchannel at the output, to accommodate an optical fiber. For imaging of the intensity profiles onto a CCD camera, L^2 devices were prepared so that there was an optically flat face at the output.

L^2 Waveguides. The fluorescent cores contained 0.1−1 mM solutions of fluorescent dye in 1:1 mixtures of dimethyl sulfoxide (DMSO; n_D = 1.479; EM Science, 99.9%) and ethylene glycol (EG; n_D = 1.431; Mallinckrodt, 99.95%). DMSO and EG were chosen because they are compatible with PDMS[25] and because they are good solvents for many organic dyes.[26] Methanol was used for the cladding liquid instead of water[2] when a nonpolar dye was present in the core liquid to avoid a precipitation of the dye due to diffusion of water into the core stream. The fluorescent dyes were fluorescein sodium salt (Aldrich ∼70%), rhodamine 6G (Aldrich, 95%), sulforhodamine B (Eastman, 99+%), and perylene (Aldrich, 99+%). Cladding solutions were 18 MΩ water (n_D = 1.331; Millipore, Milli-Q), methyl alcohol (n_D = 1.329; Aldrich, 99.9%), DMSO, or 1:1 mixtures of DMSO/EG (n_D = 1.455). Core and cladding liquids were pumped into the channels using syringes and programmable syringe pumps (Genie, Kent Scientific Corp.). Flow rates were maintained between 0.5 and 10 mL/h for each individual stream (corresponding to 1.4−28 cm/s for these channels).

Characterization. Spectroscopic measurements were carried out with a fiber-coupled UV−visible spectrophotometer (Spectral Instruments Inc.). The fluorophores were excited by irradiation, perpendicular to the microchannel plane, with a bundled fiber-optic light source (150 W, tungsten−halogen, Cuda). The light beam was focused to a 4-mm spot with a 0.25 NA microscope objective, which could be moved along the microchannel axis. Intensity measurements were taken with a photodiode (ThorLabs, DC 221). Images of the fluorescent dye streams in the microchannel (perpendicular to the waveguide axis) were taken using CCD cameras (Mintron, MTV-73K3HN; LCL Watec 902C) and a

(20) McDonald, J. C.; Duffy, D. C.; Anderson, J. R.; Chiu, D. T.; Wu, H.; Schueller, O. J.; Whitesides, G. M. *Electrophoresis* **2000**, *21*, 27−40.

(21) Berlman, I. B. *Handbook of Fluorescence Spectra of Aromatic Molecules*, 2nd ed.; Academic Press: New York, 1971.

(22) Kuhn, H. In *Biophysics*; Hoppe, W., Lohmann, W., Markl, H., Ziegler, H., Eds.; Springer-Verlag: Berlin, 1983.

(23) Yuan, J.; Wang, G.; Matsumoto, K. *Trends Inorg. Chem.* **2001**, *7*, 109−117.

(24) Stone, H. A. *Annu. Rev. Fluid Mech.* **2004**, *36*, 381−411.

(25) Lee, J. N.; Park, C.; Whitesides, G. M. *Anal. Chem.* **2003**, *75*, 6544−6554.

(26) Maeda, M. *Laser Dyes: Properties of Organic Compounds for Dye Lasers*; Academic Press: New York, 1984.

(27) Holden, M. A.; Kumar, S.; Castellana, E. T.; Beskok, A.; Cremer, P. S. *Sens. Actuators, B* **2003**, *92*, 199−207.

(28) Kamholz, A. E.; Yager, P. *Biophys. J.* **2001**, *80*, 155−160.

(29) Ternstrom, G.; Sjostrand, A.; Aly, G.; Jernqvist, A. *J. Chem. Eng. Data* **1996**, *41*, 876−879.
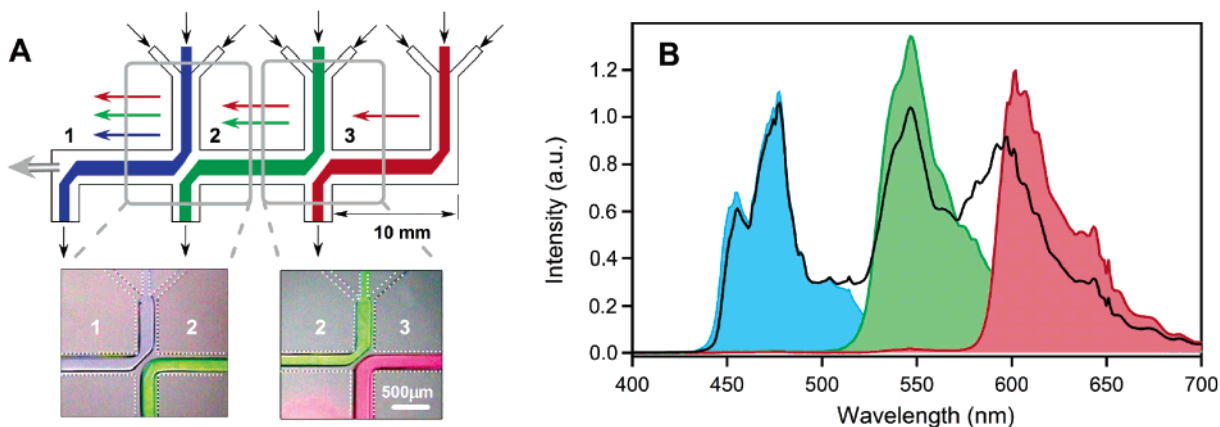
Figure 2. (A) Top-view scheme for a cascade of L^2 fluorescent light sources consisting of a series of microfluidic channels in PDMS. Multiple waveguides occupy the same central microfluidic channel. The flow of waveguide 2 displaces waveguide 3, and the flow of waveguide 1 displaces waveguide 2 at cross-junctions in the central channel. Light output is transferred between waveguides at these junctions where fluids take 90° turns. The dimensions of the central channel were 130 μm × 300 μm × 3 cm ($h \times w \times l$). Insets: Optical micrographs of the cross-junctions. The brightness and contrast have been adjusted for clarity. Dotted lines highlight the walls of the channels. (B) Spectral output (solid line) of a cascade of L^2 fluorescent light sources containing 0.5 mM solutions of perylene, fluorescein, and sulforhodamine B in DMSO/EG (1:1), when the entire central channel was irradiated with a single halogen source (uncollimated). Flow rates were 0.8, 2, and 5 mL/h for respective fluorescent cores (1, 2, and 3). Core/cladding rates were kept at a ratio of 2:1 for each waveguide. Selective illumination of discrete sections of the central microchannel with a collimated halogen source (each region of illumination was 4 mm in diameter) allowed selective excitation of individual fluorophores (colored areas).

5× microscope objective. Intensity profiles of the fluorescent light output were imaged onto CCD cameras with a 10× microscope objective.

RESULTS AND DISCUSSION

Cascade of L^2 Waveguides. We illustrate the spatial separation of dyes in separate sections of a microfluidic channel with results from a design that cascades light sources with different frequencies (Figure 2). This design was a modification of a single core L^2 waveguide (Figure 1A). The long axis of the device (horizontal in the diagram) comprised a chain of end-coupled L^2 waveguides containing liquid flowing in the laminar regime, each with a different fluorophore. The flows of liquids moved along the long axis of the device (from right to left in the diagram), that is, along the axis of the waveguide. The pressures in the inlet streams (top black arrows) were adjusted to direct the fluorescent cores into individual outlets along the main channel. The colored arrows above the long axis of the device indicate the expected spectral content in each section of the device. The transfer of fluorescent light output from adjacent waveguides occurred at cross-junctions where the fluid stream in one L^2 waveguide was displaced by another, forming a 90° bend/end couple for both waveguides. A fiber-optic spectrometer (UV−Vis spectrometer-430, SI Photonics, Inc.), end-coupled to the device (at the far left of the diagram), collected the total fluorescence output.

The cascade arrangement of the dyes with increasing fluorescence energy along the channel axis was critical in the operation of this device: this order prevented absorption of the waveguided light by the dyes emitting at low energy. A reverse arrangement of the dyes—one beginning with highest energy dye (far right channel) and terminating with the lowest energy dye (far left channel)—resulted in the removal of the blue and green components from the spectra due to near-total absorption of the high-energy fluorescence as it propagated along the L^2 waveguide.

Figure 2B displays the spectral output of a cascade of L^2 light sources under different illumination conditions. Each L^2 waveguide

had methanol ($n_D = 1.329$) in the cladding streams and a 0.5 mM fluorescent dye in DMSO/EG, 1:1 ($n_D = 1.455$) in the core stream. With this refractive index contrast, we expect that 4.3% of the light that is emitted isotropically from the dyes will be captured and guided in the forward direction of the waveguide.[2] The fluorophores in each section of the waveguide (from right to left) were perylene (blue emission), fluorescein (green emission), and sulforhodamine B (red emission). The individual colored peaks in Figure 2B are the total output of the device when only one dye was excited (by irradiating a 4-mm section of the central microchannel). The spectral output of the device, when the entire long axis was illuminated (Figure 2B, solid line), is essentially the sum of these peaks, indicating that we have eliminated absorption−reemission and resonant coupling through spatial separation of the fluorescent dyes.

The cascade of L^2 fluorescent light sources has the attractive feature that a single set of dyes can either produce a range of narrow spectral outputs by selective illumination or cover the entire visible spectrum by large-area illumination. There remain, however, some restrictions on the selection of dyes, because emissions from the low-energy dyes must always pass through another dye. Thus, the high-energy fluorophores must always be transparent at low frequencies, because high concentrations of dyes (mM, corresponding to attenuation depth of ∼100 μm) are preferred in these devices to maximize emitted optical power. In addition, the cascade system is limited to a relatively small number of dyes (<5) before the system becomes unmanageable due to the following: (i) difficulties illuminating the entire system; (ii) difficulties in maintaining fluid pump ratios to give good interfaces at the cross-junctions for waveguide coupling; and (iii) difficulties associated with the decrease in output efficiency as the low-energy dyes are moved farther away from the output of the device (and thus multiplying the losses associated with end-coupling).

Arrays of L^2 Waveguides. An alternative to the cascade design is an array design, which removes these difficulties by
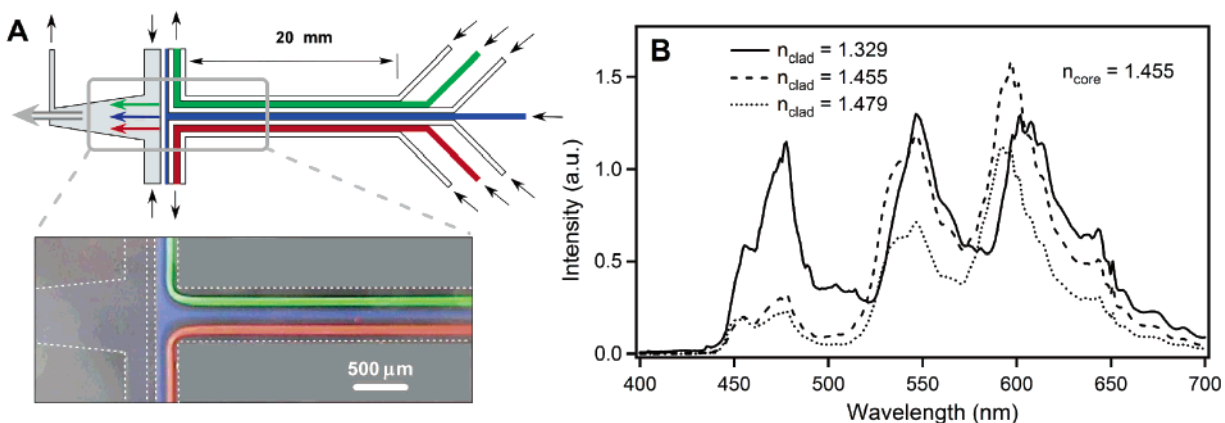
Figure 3. (A) Top-view scheme for the array of L^2 fluorescent light sources, consisting of parallel L^2 waveguides in a single PDMS microchannel. An end-coupled, tapered, liquid-core waveguide filled with DMSO collected the total fluorescence output. Inset: Optical micrograph of the T-junction. Dotted lines outline the walls of the PDMS channels. (B) Spectral output (solid line) from an array of L^2 fluorescent light sources containing 0.5 mM solutions of perylene, fluorescein, and sulforhodamine B in DMSO/EG (1:1), with various cladding liquids: methanol ($n_{cladding} < n_{core}$); DMSO/EG (1:1, $n_{cladding} = n_{core}$); DMSO ($n_{cladding} > n_{core}$). Flow rates for all inputs were held constant at 4 mL/h each.

treating multiple fluorescent cores equivalently (Figure 3). Here, adjacent, dye-containing core streams share cladding streams along their long axis, and fluorescent emission from each dye remains separate and does not travel along any section of the waveguide containing another dye. This design can, in principle, accommodate several fluorescent L^2 streams without increasing the overall length of the waveguide channel.

A typical array of liquid waveguides with multiple core streams was several hundred of micrometers wide (allowing a channel height of ~130 μm and an aspect ratio of ~1 for each liquid stream). For spectroscopic characterization (and potential applications), it was necessary to merge the light outputs of all of the L^2 waveguides in the array, so that they could be fed into a single 125-μm optical fiber (or analyte compartment). A tapered, spatially distinct, liquid waveguide was end-coupled to the waveguide array (the channel ends in a T split) and acted as an adapter to combine the emissions of the parallel waveguides, concentrating them on an optical fiber. The tapered liquid waveguide contained a stationary liquid with index of refraction higher than PDMS (e.g., DMSO, $n_D = 1.479$) and ensured that light from each of the L^2 waveguides in the array reached the end-coupled optical fiber.

A fiber-optic spectrometer measured the total fluorescence from the L^2 waveguide array. The overall spectral characteristics (solid line in Figure 3B) were similar to those of the cascade device, in terms of both the relative intensity distribution between the peaks and the overall intensity. Good optical isolation of individual fluorescent light sources is manifested in equal intensity of their corresponding peaks. Unlike the cascade design, individual dyes could not be selectively illuminated; however, tuning of the spectral output was possible through regulation of dye flows and concentrations, including removal of selected dye(s) from the array. An increase (decrease) in the relative flow rate of a dye in the array results in the higher (lower) volume fraction of this dye in the channel and, subsequently, increased (decreased) light output in that particular part of the spectrum. Stopping the flow of one of the liquid cores resulted in omission of the corresponding peak from the combined spectrum.

Although we expected the lateral isolation of the fluorescence in arrays using a methanol core to be essentially complete (i.e., decay length of the evanescent field ≪ size of the cladding), we

observed a dependence of the combined spectra on the exact ordering of the fluorescent cores in the channel. We tested two hypotheses that might explain the phenomenon responsible for this unexpected behavior: (i) The mutual diffusion of the core and cladding fluids might wash out the refractive index contrast in the waveguide and thus degrade the optical isolation; (ii) the passing of the light output from outermost waveguides through a small thickness of the central core when it splits at the T (Figure 3A) might lead to absorption by the dye in the central core. Changing the flow rates and relative size of the core/cladding streams did not substantially alter the form of the spectrum (see also a discussion below on diffusion effects). We did, however, observe substantial reduction in the output of the side L^2 waveguides, when they emitted at wavelengths that were susceptible to absorption by the central liquid core. For example, when the central core contained sulforhodamine B, the combined emission was predominantly red, and when the central core contained fluorescein, only the blue emission lost substantial intensity. These observations are indeed consistent with the expected level of absorption, since the concentrations of the dyes were adjusted to provide absorbance of ~1 for path lengths on the order of 100 μm. We conclude that passing light through a highly absorbing liquid core at the exit aperture of the array is responsible for the reduction in light output at long wavelength. Therefore, arrays of fluorescent L^2 waveguides should be constructed in such a way as to minimize this absorption by positioning dyes emitting at higher energy closer to the central axis of the array.

Refractive Index Contrast and Light Confinement. The characteristics of the waveguide array also could be controlled by modification of the refractive index contrast ($\Delta n = n_{core} - n_{cladding}$). Figure 3B displays the spectra obtained from a three-dye, array-based device containing 0.5 mM solutions of perylene, sulforhodamine B, and fluorescein in DMSO/EG (1:1). When the refractive index of the cladding ($n_{cladding}$) was well below that of the core (n_{core}) (methanol, $n_D = 1.329$), there was negligible energy transfer between the dyes, as evident in the equivalent intensities of each dye in the output spectrum. As the refractive index of the cladding increased (DMSO/EG, 1:1, $n_D = 1.455$, and DMSO, $n_D = 1.479$) so did the coupling.
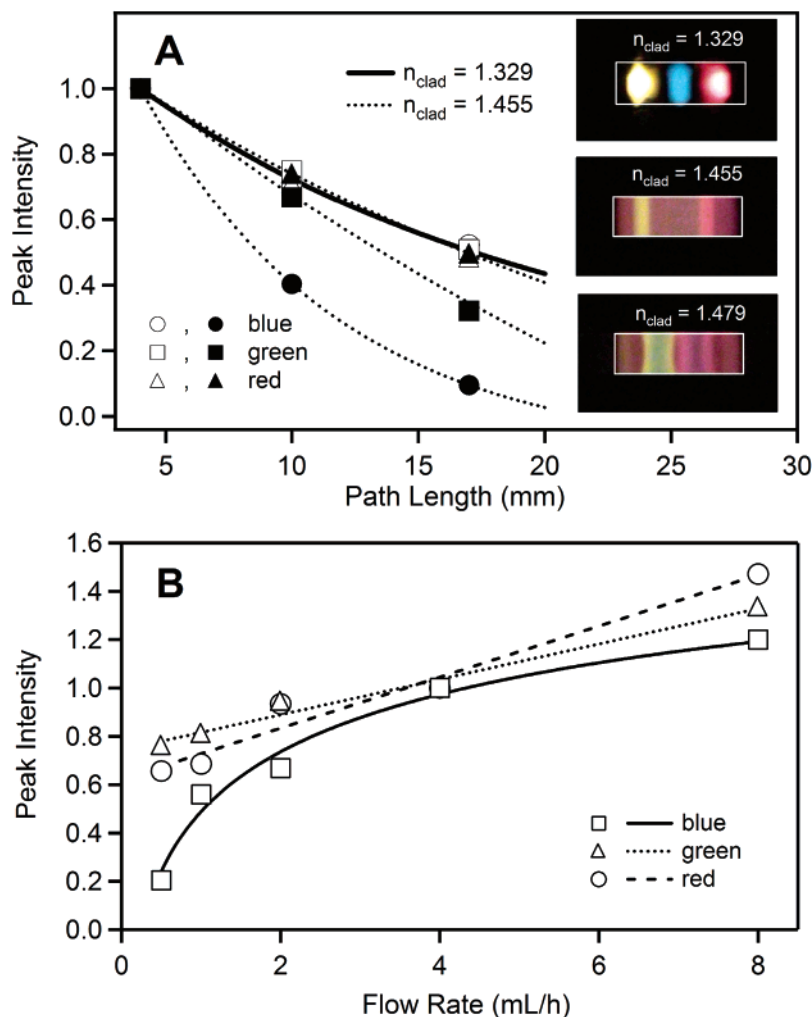
Figure 4. (A) Maximum intensity for each peak (normalized to the intensity at 5-mm path length) versus path length for the array of L^2 light sources (dye solutions are the same as those in Figure 3; $n_{core} = 1.455$). The path length was defined by the distance from the center of the optically pumped area (a 4-mm diameter circle) to the exit T-junction. Insets: Cross-sectional views of the array output imaged on a CCD camera. For imaging, the device was prepared with an optically smooth window after the T-junction, instead of a tapered liquid-core waveguide. White rectangles outline the cross section of the microchannel for clarity. (B) Maximum intensity for each peak (normalized to the intensity at 4 mL/h) versus flow rate for the array of L^2 light sources (the same dye solutions as in Figure 3 and methanol cladding). The flow rate indicates the rate of each individual stream (the rates of the three liquid core streams and four cladding streams are equal).

In all cases ($n_{cladding} < n_{core}$, $n_{cladding} = n_{core}$, $n_{cladding} > n_{core}$), the dyes and cores were confined by laminar flow; thus, the relative refractive indices of the liquids in adjacent flows determined the optical confinement within the array (although effects of diffusion become pronounced at low flow rates—see below). When $\Delta n = 0.126$, we found negligible energy transfer, since the Δn was large enough that the evanescent wave for a given waveguide did not extend appreciably into the adjacent waveguide. When $\Delta n = 0$, we expected no confinement of the fluorescence, except by the walls of the PDMS microchannel ($n_D = 1.406$). Although resonant energy transfer was not possible because the dyes were physically separated, there was substantial absorption and reemission, which diminished the output of the high-energy dyes. Interestingly, when $\Delta n = -0.024$, there was also an appreciable decrease in the output intensity of the higher energy dyes. In this case, the fluorescent output was not completely confined to the dyed core streams, but diffused into the cladding streams. Although the light should be largely confined to a dye-free cladding stream, the evanescent field extended into the dye-

containing streams, leading to appreciable absorption−reemission. For the two cases where $\Delta n \leq 0$, the output for the perylene was most diminished by the effects of absorption−reemission, because (i) it is the dye with the highest energy fluorescence and (ii) its location in the central waveguide make possible the coupling to both rhodamine- and fluorescein-containing cores.

We confirmed the interpretation of cross-waveguide coupling by imaging the distribution of fluorescent light at the terminus of the array and determining attenuation characteristics of the array. The presence of energy-transfer processes will be more pronounced at long path lengths. Figure 4A displays a plot of the intensity of the peaks for each dye versus the path length from the center of the optical pumping zone to the exit aperture (T-junction) of the microchannel. Peak intensities were normalized with respect to their intensity at a path length of 4 mm. For $\Delta n = 0.126$ (fully decoupled waveguides), although the peak intensities decreased ~50% as the channel length increased from 4 to 17 mm, the relative peak intensities remained the same for all wavelengths, independent of the path length. For $\Delta n = 0$ (fully
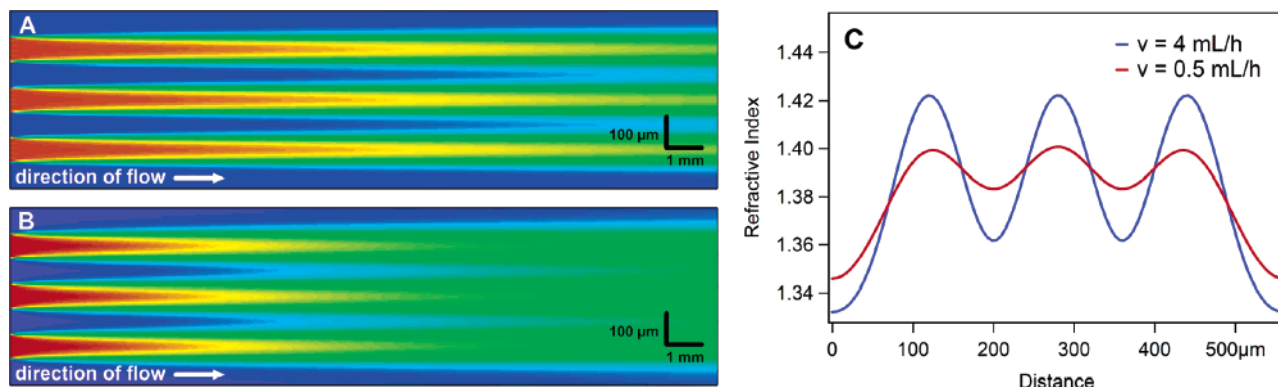
Figure 5. (A, B) Simulation of refractive index distribution in a two-dimensional, 0.56 × 20 mm ($w \times l$), L^2 waveguide as function of the flow rate: 4 (A) and 0.5 mL/h (B). The diffusion coefficient used in the simulation was 10^{-9} m²/s. The refractive indices of the two liquids were 1.455 (red, DMSO/EG 1:1) and 1.329 (blue, methyl alcohol). The direction of flow was from left to right. (C) Cross sections of the refractive index profiles at the ends of the simulated channels (20-mm distance from inlets) are displayed for direct comparison.

coupled waveguides), there was a greater decrease in peak intensities (as large as 90%) for peaks at shorter wavelength (blue and green), whereas the peak in the red part of the spectrum showed the same attenuation as in the fully decoupled waveguide array. The differences between the blue, green, and red peaks can be rationalized by a higher fraction of energy transfer for longer paths, with energy transfer taking place in the order, blue (perylene) to green (fluorescein) and red (sulforhodamine B), and green to red.

The insets of Figure 4A display images of the output cross section taken with a color CCD camera focused trough a microscope objective onto the T-junction of the microchannel. Clear indications of energy transfer from the high-energy dye (perylene) to the lower energy dyes (rhodamine and fluorescein) are apparent in the $\Delta n \leq 0$ systems, where the blue color is no longer visible. The $\Delta n > 0$ system is the only case where all fluorescence outputs are well confined.

Diffusion Effects. The refractive index contrast of a L^2 waveguide is influenced by diffusion, and spectral output depends on the residence time of the dye in the microchannel.[17] The difference in refractive index between the liquid core and liquid cladding will decrease as the liquids flow and mix (by lateral diffusion) along the length of the channel. This diffusive mixing makes flow rate an important factor in the performance of the waveguides. Figure 4B displays a plot of peak intensities versus the flow rate for each dye at a fixed optical-pumping path length of 4 mm. As the flows slowed, diffusion increased, and Δn decreased. Below a critical flow rate (~1 mL/h or ~ 3 cm/s in a 2-cm-long channel), Δn was no longer sufficient to prevent cross-talk between parallel waveguides, and the output intensity for the high-energy dyes decreased.

Figure 5 summarizes the results of a simulation of diffusive mixing at two different flow rates in the microchannel (see Appendix for the solution of differential equations for diffusion involving multicore arrays a microchannel and details on the calculations). The initial refractive indices (far left) were 1.455 (red) and 1.329 (blue). The dimensions of the two-dimensional simulated microchannel were 0.56 × 20 mm. At a relatively high flow rate (4 mL/h), the refractive index profile (Figure 5C) at the end of the 2-cm microchannel remains well defined. This profile provides an NA of 0.41 and will theoretically guide 3% of light emitted isotropically from the fluorophores in that portion

of the waveguide. This percentage is calculated from the following expression: $\Delta n/(2n_{core})$ (see ref 2 for derivation). At a relatively low flow rate (0.5 mL/h), the dynamic range of the refractive index profile at the end of the microchannel is dramatically decreased (i.e., diffusive mixing equalizes the composition if the core/cladding streams and, thus, decreases n_{core} and increases $n_{cladding}$ to give a decreased Δn). This graded index profile gives a decreased NA of 0.20 and will theoretically guide only 0.8% of the light emitted by the fluorophores. In addition, with such a low value of Δn in graded-index waveguide, the optical path of light that is contained within the core of one waveguide will extend into adjacent fluorescent cores.

CONCLUSIONS

The broadband light sources described here, in principle, should allow arbitrary permutations of dye solutions and should give a high degree of control over the optical output. We expect the availability of prealigned, broadband light sources to be useful for spectroscopy in microfluidic systems. Arrays and cascades of L^2 light sources, in general, have several features that are potentially useful for applications in microsystems: (1) L^2 light sources generate intensity comparable to standard fiber-optic spectrophotometer-based light sources. (2) L^2 light sources are not restricted by the size requirements imposed by fiber-optic light sources. (3) L^2 light sources arranged as arrays and cascades eliminate energy transfer between multiple fluorophores and yield broadband spectral output. (4) L^2 light sources have all of the flexibility associated with L^2 waveguides—their size, geometry, and chemical composition can be tuned through changes in flow rates or selection of liquids. (5) L^2 light sources are fabricated in moldable elastomers and are entirely amenable to rapid proto-typing.[18−20] The primary disadvantage of these systems is the requirement to manipulate liquids using pumps and reservoirs.

APPENDIX

Effects of Diffusion on Index of Refraction in Arrays of L^2 Waveguides. The two-dimensional (length−width) refractive index profile in the channel, $n(x,y)$, can be derived from the
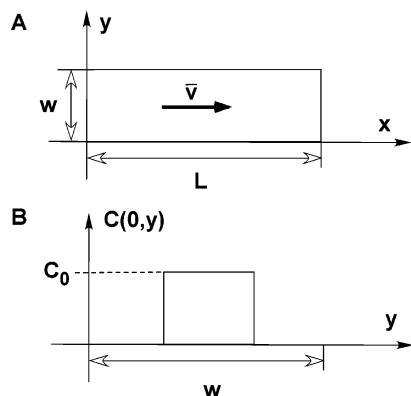
Figure 6. (A) Diagram of the channel geometry considered in two-dimensional convective−diffusive transport in a microchannel having width w and length L. (B) Concentration profile at the input of the channel ($x = 0$).

concentration profile of the m liquid components (f is the volume fraction):

$$n(x,y) = \sum_{i=0}^{m} f_i(x,y)\, n_i \qquad (1)$$

The convective−diffusive transport for each component in incompressible fluid flow in a microchannel (Figure 6) is governed by the equation

$$\frac{\partial C}{\partial t} + \bar{v}\nabla C = D\nabla^2 C \qquad (2)$$

where C is the concentration, D a is the mass diffusivity, w is the characteristic length (width of the channel), and $\bar{v}$ is the velocity vector. Assuming that the densities of liquids are approximately equal, the (molar) concentration C in eq 2 can be understood as a volume fraction f. Equation 2 can be significantly simplified under several assumptions/considerations:[27,28] (1) for steady-state flow, $\partial C/\partial t = 0$; (2) for fully developed flow, $\partial v/\partial x = 0$; (3) the velocity component along Y (normal to the long axis of the channel) is negligible except at the inlets and outlet, so that $|\bar{v}| \approx v_x = v$, where v is the average fluid velocity; and (4) since the concentration gradient is significantly lower along the channel than across it, the diffusion along X is negligible compared to diffusion along Y; i.e., $\partial^2 C/\partial x^2 \ll \partial^2 C/\partial y^2$.

Equation 2 then reduces to

$$v\frac{\partial C}{\partial x} = D\frac{\partial^2 C}{\partial y^2} \qquad (3)$$

This equation can be written in dimensionless coordinates:

$$\frac{\partial C}{\partial X} - \frac{\partial^2 C}{\partial Y^2} = 0 \qquad (4)$$

where

$$X = (1/Pe)x/w$$

$$Y = y/w \qquad (5)$$

w is the width of the channel and Pe is the Peclet number:

$$Pe = D/vw \qquad (6)$$

The analytical solution to the differential equation (4) can be obtained by separation of variables under the following boundary conditions:

$$\frac{\mathrm{d}C}{\mathrm{d}y}\big|_{x=0} = \frac{\mathrm{d}C}{\mathrm{d}y}\big|_{x=w} = 0$$

$$C(0,y) = C_0(y)$$

$$C(\infty,y) = \frac{1}{w}\int_0^w C_0(y)\,\mathrm{d}y \qquad (7)$$

The general solution is given by

$$C(X,Y) = C(\infty,Y) + \sum_{n=0} A_n e^{-(\pi n)^2 X}\cos(\pi n Y) \qquad (8)$$

The value of coefficients in eq 8 can be established by multiplying both parts of eq 8 by $\cos(\pi k Y)$ and integrating over the width of the channel at $X = 0$ (only the term $k = n$ remains):

$$A_n = 2\int_0^1 (C(0,Y) - C(\infty,Y))\cos(\pi n Y)\,\mathrm{d}Y \qquad (9)$$

For a rectangular initial concentration profile ($C_0(y) = C_0$ for $a < y < b$, and $C_0(y) = 0$ otherwise), the A_n coefficients are

$$A_n = \frac{2}{\pi n}C_0\left(\sin\left(\pi n \frac{b}{w}\right) - \sin\left(\pi n \frac{a}{w}\right)\right) \qquad (10)$$

and

$$C(\infty,y) = C_0\frac{b-a}{w}$$

For multiple rectangular profiles of the same component (as in L^2 waveguide array of the type shown in Figure 1B), the total concentration can be found by adding results of the concentration profile found from eqs 8 and 10. Diffusion coefficients for the methanol/ethylene glycol system were assumed to be similar to those found in water/ethylene glycol systems.[29]